The Company of Biologists

RESEARCH REPORT

MEF2C regulates outflow tract alignment and transcriptional control of *Tdgf1*

Ralston M. Barnes[1,*], Ian S. Harris[1,2,*], Eric J. Jaehnig[1], Kimberly Sauls[3], Tanvi Sinha[1], Anabel Rojas[1], William Schachterle[1], David J. McCulley[1], Russell A. Norris[3] and Brian L. Black[1,4,‡]

ABSTRACT

Congenital heart defects are the most common birth defects in humans, and those that affect the proper alignment of the outflow tracts and septation of the ventricles are a highly significant cause of morbidity and mortality in infants. A late differentiating population of cardiac progenitors, referred to as the anterior second heart field (AHF), gives rise to the outflow tract and the majority of the right ventricle and provides an embryological context for understanding cardiac outflow tract alignment and membranous ventricular septal defects. However, the transcriptional pathways controlling AHF development and their roles in congenital heart defects remain incompletely elucidated. Here, we inactivated the gene encoding the transcription factor MEF2C in the AHF in mice. Loss of *Mef2c* function in the AHF results in a spectrum of outflow tract alignment defects ranging from overriding aorta to double-outlet right ventricle and dextro-transposition of the great arteries. We identify *Tdgf1*, which encodes a Nodal co-receptor (also known as Cripto), as a direct transcriptional target of MEF2C in the outflow tract via an AHF-restricted *Tdgf1* enhancer. Importantly, both the *MEF2C* and *TDGF1* genes are associated with congenital heart defects in humans. Thus, these studies establish a direct transcriptional pathway between the core cardiac transcription factor MEF2C and the human congenital heart disease gene *TDGF1*. Moreover, we found a range of outflow tract alignment defects resulting from a single genetic lesion, supporting the idea that AHF-derived outflow tract alignment defects may constitute an embryological spectrum rather than distinct anomalies.

KEY WORDS: MEF2, *Tdgf1*, Cripto, Enhancer, Heart development, Mouse

INTRODUCTION

Congenital heart defects are the most common birth defects in humans, affecting ~0.8% of all live births, and defects in the alignment of the cardiac outflow tracts (OFTs) cause a diverse group of serious cyanotic malformations (Anderson et al., 1974; Hoffman and Kaplan, 2002). Cells from the anterior second heart field, also referred to as the anterior heart field (AHF), are added to the arterial pole of the heart after its initial formation and form all of the mesoderm-derived components of the cardiac OFT and the majority

of the right ventricle (RV) (Black, 2007; Kelly, 2012). The addition of cells from the AHF is likely to provide the embryological basis for OFT alignment and membranous septal defects (Neeb et al., 2013). However, despite the identification of the AHF and its role in OFT development, the transcriptional and signaling pathways that function in this progenitor population and its derivatives and the possible involvement of these pathways in congenital heart defects remain incompletely elucidated.

The MADS box transcription factor MEF2C is a key component in the network regulating AHF development (Black, 2007; Dodou et al., 2004). The *Mef2c* gene is required for heart development in the mouse, and mice that lack *Mef2c* die around embryonic day (E) 10.0 due to failure in cardiac morphogenesis and a failure of the heart to undergo rightward looping (Lin et al., 1997). This morphogenetic defect has been interpreted as a failure of cells from the AHF to be properly deployed to the heart (Nakazawa et al., 2011; Verzi et al., 2005). *MEF2C* has also been associated with congenital OFT defects in human patients (Kodo et al., 2012), but the specific function and transcriptional targets of MEF2C in the AHF and its derivatives are largely unknown.

Teratocarcinoma-derived growth factor 1 (TDGF1; also known as Cripto) is a Nodal signaling co-receptor (Ding et al., 1998; Schier and Shen, 2000). Nodal is a TGFβ family member ligand that signals through core TGFβ receptors in association with an additional co-receptor of the EGF-CFC family, such as TDGF1, to activate downstream intracellular signaling (Shen and Schier, 2000). *Tdgf1*-null mouse embryos exhibit striking defects in mesoderm formation and anterior-posterior patterning, resulting in early embryonic lethality and concomitant absence of cardiac marker gene expression (Ding et al., 1998; Xu et al., 1999). Recent studies identified mutations in human *TDGF1* associated with isolated congenital heart defects, including membranous ventricular septal defects and conotruncal alignment defects (Roessler et al., 2008; Wang et al., 2011), suggesting that errors in this component of Nodal signaling might be involved in developmental defects that are restricted to cardiac development.

To define pathways downstream of MEF2C important for the development of the AHF and its derivatives, we inactivated *Mef2c* exclusively in the AHF and found that *Mef2c* AHF knockout mice die at birth with severe cyanosis, ventricular septal defects and a spectrum of OFT alignment defects. *Tdgf1* expression was completely abolished in the OFT in the absence of MEF2C, and we identified a transcriptional enhancer from *Tdgf1* with activity that completely mimics endogenous *Tdgf1* expression in AHF derivatives. Importantly, we found that the *Tdgf1* AHF enhancer is a direct transcriptional target of MEF2C via a conserved consensus MEF2 site in the enhancer. Thus, these studies establish a requirement for MEF2C for OFT development and define a direct transcriptional pathway between MEF2C and the congenital heart disease gene *Tdgf1*.

[1]Cardiovascular Research Institute, University of California, San Francisco, San Francisco, CA 94143-3120, USA. [2]Division of Cardiology, University of California, San Francisco, San Francisco, CA 94143, USA. [3]Cardiovascular Developmental Biology Center, Medical University of South Carolina, Charleston, SC 29425, USA. [4]Department of Biochemistry and Biophysics, University of California, San Francisco, San Francisco, CA 94143, USA.
*These authors contributed equally to this work

‡Author for correspondence (brian.black@ucsf.edu)

DEVELOPMENT

RESULTS AND DISCUSSION
MEF2C is required for proper OFT alignment

We deleted *Mef2c* exclusively in the AHF and its derivatives using *Mef2c*-AHF-Cre (Verzi et al., 2005) (Fig. S1). This approach resulted in a greater than 98.5% reduction of *Mef2c* transcripts in the RV and OFT by E10.5 (Fig. S1). Mice with deletion of *Mef2c* in the AHF (referred to hereafter as *Mef2c*[AHF-KO] or CKO) were born at the expected Mendelian frequency (Fig. S1), but approximately half displayed profound cyanosis and died shortly after birth. Control neonates showed normal positioning of the outflow vessels and proper septation of the ventricles (Fig. 1A). By contrast, 21/36 of *Mef2c*[AHF-KO] mice that were examined in detail had significant cardiac defects, ranging from isolated membranous ventricular septal defect (VSD) to more extensive OFT alignment defects with associated VSD (Fig. 1, Table 1). The spectrum of OFT alignment defects observed in *Mef2c*[AHF-KO] mice included overriding aorta with stenotic or atretic pulmonary artery and associated membranous VSD (Fig. 1B), reminiscent of the defects observed in

human patients with tetralogy of Fallot (Anderson et al., 2013). A significant number of neonatal *Mef2c*[AHF-KO] mice also presented with transposition of the great arteries (TGA; Fig. 1C) and double-outlet right ventricle (DORV; Fig. 1D).

Mef2c[AHF-KO] neonates displayed nearly completely penetrant abnormalities in the semilunar valve leaflets, even in the absence of other obvious defects (Fig. 1, Table 1), suggesting that MEF2C might play a role in endocardial cushion maturation and valve development. Alternatively, disrupted blood flow might have created hemodynamic alterations in *Mef2c*[AHF-KO] fetuses, leading to the observed valve dysmorphogenesis (Menon et al., 2015). To examine the semilunar valves in additional detail, we created 3D reconstructions of the OFTs in *Mef2c*[AHF-KO] and control neonates and measured the volume of the valve leaflets and the length of the OFT vessels. The volume of the aortic valve leaflets was significantly smaller in *Mef2c*[AHF-KO] mice than in controls [control, 1.00 ± 0.22 ($n=6$); *Mef2c*[AHF-KO], 0.58 ± 0.16 ($n=7$); $P=0.006$; values are relative mean volume±s.d.; see also renderings of 3D
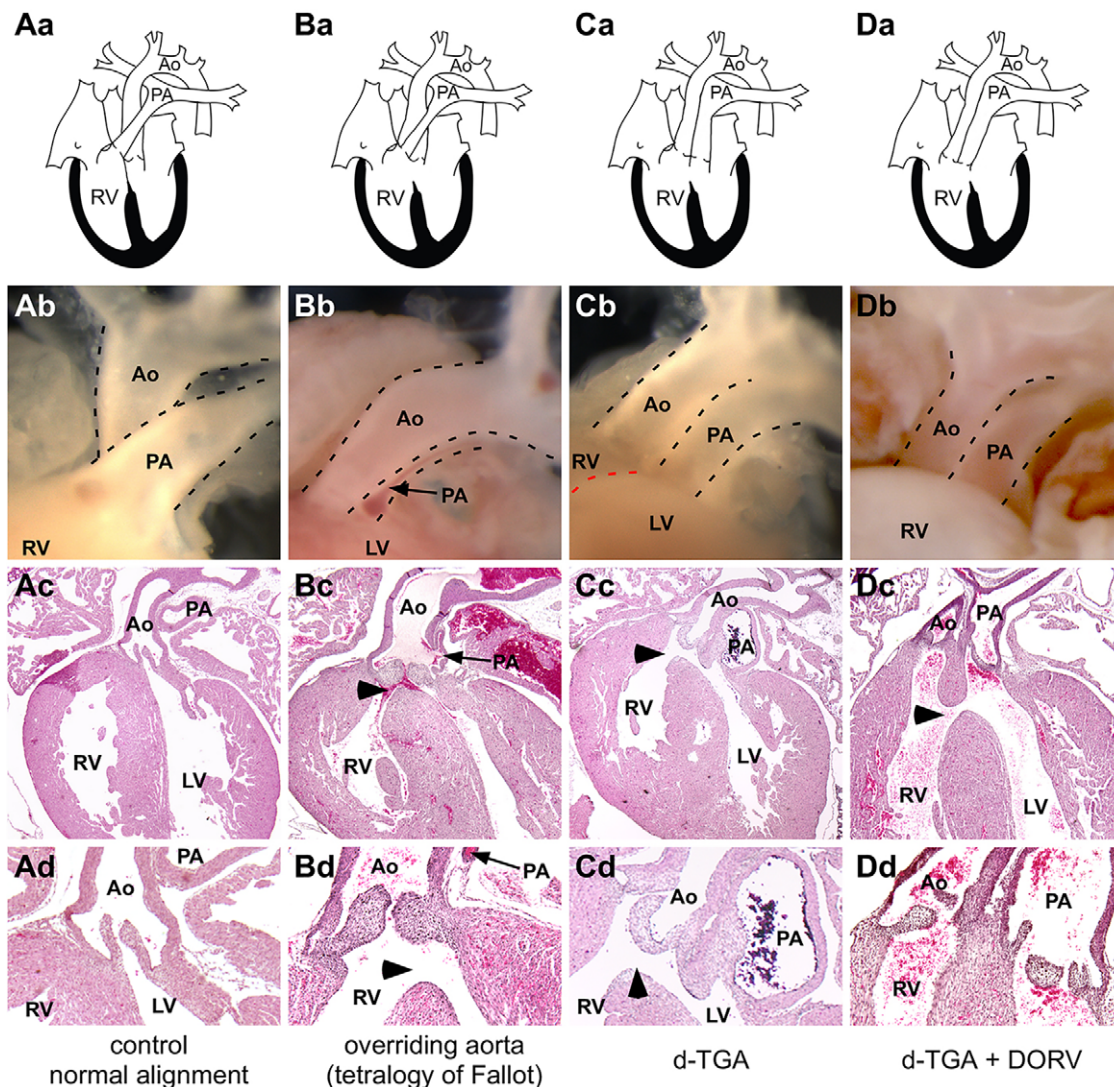

Fig. 1. *Mef2c* function in the AHF is required for proper OFT alignment. (Aa-d) Normal alignment of the aorta (Ao) and pulmonary artery (PA) in control neonatal mice. RV, right ventricle; LV, left ventricle. (B-D) Subsets of *Mef2c*[AHF-KO] neonatal mice displayed a tetralogy of Fallot-like phenotype, including hypoplastic pulmonary artery, ventricular septal defect (VSD, arrowheads), overriding aorta, and hypertrophic right ventricle (Ba-d); dextro-transposition of the great arteries (d-TGA) with VSD (Ca-d); or double-outlet right ventricle (DORV) with or without d-TGA (Da-d). Note that all *Mef2c*[AHF-KO] mice displayed thickened and club-shaped semilunar valves, as shown in Bd-Dd.

Table 1. Penetrance of the spectrum of phenotypes in *Mef2c*[AHF-KO] neonates

Genotype	n	Normal	Isolated OFT valve defects	OFT valve defects associated with:			
				VSD only	VSD+overriding aorta (ToF-like)	VSD+DORV	VSD+d-TGA
Mef2c-AHF-Cre[Tg/0];*Mef2c*[flox/−] (CKO)	36	1	14	8	5	3	5
Mef2c[flox/+] (wt)	4	4	0				
Mef2c[flox/−]	5	5	0				
Mef2c-AHF-Cre[Tg/0];*Mef2c*[flox/+] (het)	13	13	0				

For each neonate, transverse sections were cut through the entire heart and phenotypes were catalogued in a blinded fashion. CKO, *Mef2c*[AHF-KO] conditional knockout; het, *Mef2c*[AHF-KO] heterozygous; wt, wild type; OFT, outflow tract; VSD, membranous ventricular septal defect; ToF, tetralogy of Fallot; DORV, double-outlet right ventricle; d-TGA, dextro-transposition of the great arteries.

reconstructions in Fig. S2]. We also found that the aorta was significantly shorter in *Mef2c*[AHF-KO] mice than in controls [control, 245±28 (n=6); *Mef2c*[AHF-KO], 139±50 (n=7); Student's t-test, P=0.005; values are mean pixel length±s.d.].

The phenotypic variability seen in *Mef2c*[AHF-KO] mice is intriguing, and there are several possible explanations. These experiments were conducted in a mixed genetic background, suggesting that modifier genes might influence the penetrance or severity of the phenotype (Doetschman, 2009). We believe that this is the most likely explanation for the phenotypic variability. It is also possible that the precise timing or pattern of Cre excision of *Mef2c* may have varied among embryos. However, we consider this unlikely since excision was already essentially complete in the OFT and RV by E10.5 (Fig. S1). More generally, our observations support the idea that a single primary genetic lesion can result in a range of OFT defects, which in clinical practice are often considered discrete entities (Dorfman and Geva, 2006; Johnson, 2010). Our data also support the idea that complex alignment phenotypes might form a continuous spectrum of related OFT alignment disorders, as others have also proposed based on observations from other mouse genetic models, particularly for *Tbx1* and related pathways (Brown et al., 2004; Racedo et al., 2015; Rana et al., 2014; Vincentz et al., 2005).

Tdgf1 is a direct transcriptional target of MEF2C in the developing OFT

Analyses of *Mef2c*[AHF-KO] embryos showed the first evidence of an OFT alignment phenotype at E12.5, when disruptions of the normal relationship of the aorta and the pulmonary artery to each other could be seen in ~50% of *Mef2c*[AHF-KO] embryos (Fig. S3). To gain additional insight into the cellular or molecular basis of the OFT alignment defects seen in *Mef2c*[AHF-KO] mice, we analyzed gene expression, apoptosis, proliferation, and the contribution of the *Mef2c*-AHF-Cre lineage to the heart in *Mef2c*[AHF-KO] and control embryos at E10.5 (Fig. S4). By this stage, *Mef2c*[AHF-KO] embryos had no detectable *Mef2c* expression in the OFT, but this was still just prior to the onset of any obvious OFT defects. We observed no statistically significant changes in apoptosis or proliferation between *Mef2c*[AHF-KO] and control embryos, nor did we observe any apparent differences in the contribution of the *Mef2c*-AHF-Cre lineage (Fig. S4). To gain insight into changes in gene expression in *Mef2c*[AHF-KO] mutants, we performed RNA-seq on OFTs isolated from E10.5 wild-type and mutant embryos. These results identified *Tdgf1* as the single most dysregulated gene, being reduced by ~98% in the OFTs of *Mef2c*[AHF-KO] embryos in RNA-seq (wild type, 92 FPKM; *Mef2c*[AHF-KO], 2 FPKM; Student's t-test, P<0.001). This result was confirmed by qPCR (wild type, 1.00±0.25; *Mef2c*[AHF-KO], 0.0066±0.0019; ±s.d.; n=8 each; Student's t-test, P<0.001).

The nearly complete dependence of *Tdgf1* expression in the OFT on the transcription factor MEF2C suggested the possibility of a direct transcriptional relationship. Therefore, we scanned the *Tdgf1* locus for putative transcriptional enhancers using a combination of bioinformatics approaches and analyses of open chromatin (Dubchak and Ryaboy, 2006; Thurman et al., 2012). This led to the identification of a single transcriptional enhancer in the *Tdgf1* locus with robust activity in the derivatives of the AHF (Fig. 2). Importantly, β-galactosidase activity directed by the *Tdgf1* AHF enhancer (Fig. 2H-J) was consistent with endogenous *Tdgf1* transcript expression (Fig. 2B-D) and almost perfectly mimicked the β-galactosidase activity directed by a *Tdgf1*[lacZ] knock-in allele (Ding et al., 1998; Fig. 2E-G), suggesting that we had identified a bona fide *Tdgf1* enhancer sufficient to recapitulate *Tdgf1* expression in the heart during the time when the AHF is contributing to the development of the RV and OFT.

Crossing mice harboring a stable *Tdgf1* enhancer-*lacZ* transgene, referred to as *Tdgf1::lacZ* (Fig. 2A), onto a *Mef2c*-null background resulted in loss of transgene expression (Fig. 3A,B), indicating that the enhancer was completely dependent on MEF2C for activity. Similarly, expression from the endogenous *Tdgf1* locus was also dependent on MEF2C (Fig. 3C,D). Importantly, the *Tdgf1* AHF enhancer contains a single, perfect consensus MEF2 binding site (Fig. 2A), and this MEF2 site was specifically bound by MEF2C in EMSA (Fig. 3E). Furthermore, mutation of the MEF2 site in the context of the full-length *Tdgf1* enhancer almost completely abolished enhancer activity in transgenic embryos *in vivo* (Fig. 3F,G). Taken together, these data establish that MEF2C directly regulates *Tdgf1* expression in the AHF and its derivatives via the MEF2 site in the enhancer.

The *Tdgf1* enhancer sequence also contains three consensus NKE sequences that have been previously suggested, based on *in vitro* studies, to function as NKX2-5 binding sites (Behrens et al., 2012). However, neither mutation of the three NKE elements in the *Tdgf1* enhancer nor crossing *Tdgf1::lacZ* onto an *Nkx2-5*-null background had a discernible effect on transgene expression (data not shown), suggesting that NKX2-5 is not required for *Tdgf1* enhancer function *in vivo*.

Implications of a *MEF2C-TDGF1* pathway for congenital heart disease

Importantly, the data presented here establish a direct transcriptional relationship between two genes associated with OFT alignment defects (Kodo et al., 2012; Roessler et al., 2008; Wang et al., 2011). This direct transcriptional relationship suggested the possibility that *Mef2c* and *Tdgf1* might exhibit a genetic interaction. To test this idea explicitly, we intercrossed *Mef2c*^{+/−} and *Tdgf1*^{+/−} mice to generate compound heterozygotes. Interestingly, *Mef2c*^{+/−};*Tdgf1*^{+/−} double-heterozygous mice were viable and presented with no apparent congenital heart defects (Table S1). The lack of an overt phenotype might be because double heterozygosity does not eliminate *Tdgf1*
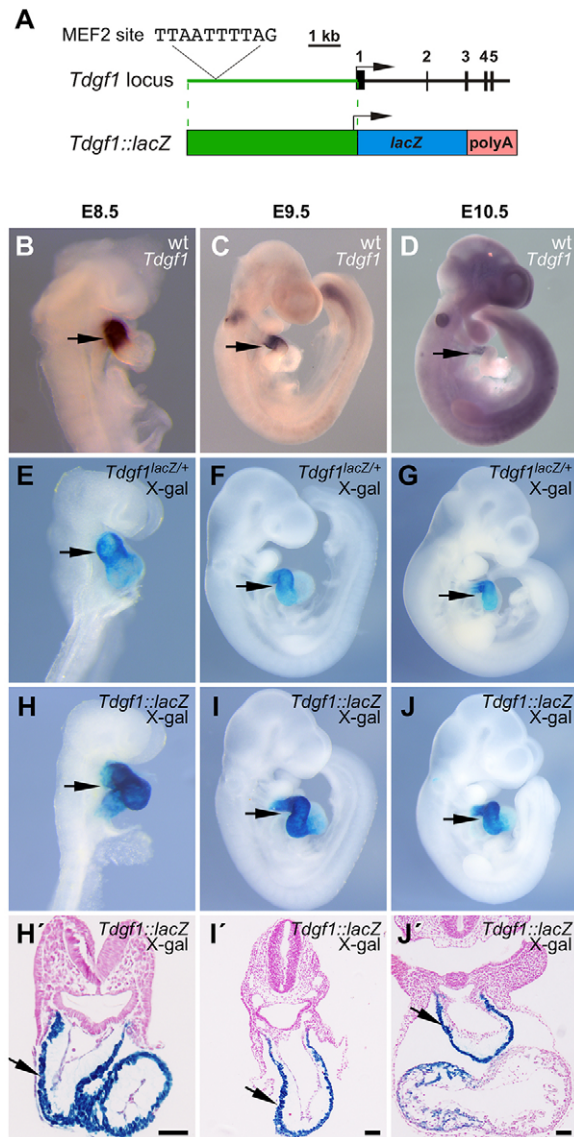
Fig. 2. *Tdgf1* is expressed in the AHF and the activity of a cardiac-specific enhancer mimics endogenous expression. (A) The murine *Tdgf1* locus and *Tdgf1::lacZ* reporter transgene. The canonical MEF2 binding site in the enhancer is indicated. Exons are numbered. (B-D) Whole-mount *in situ* hybridization for *Tdgf1* in wild type (wt) at E8.5 (B), E9.5 (C), E10.5 (D). (E-G) X-gal staining of *Tdgf1^lacZ/+* embryos also shows endogenous expression of *Tdgf1* from the knock-in allele at E8.5 (E), E9.5 (F), E10.5 (G). (H-J) X-gal-stained embryos of a stable *Tdgf1::lacZ* transgenic line at E8.5 (H,H′), E9.5 (I,I′), E10.5 (J,J′). (H′-J′) Transverse sections of X-gal-stained *Tdgf1::lacZ* transgenic embryos. Arrows indicate the OFT in all panels. Scale bars: 100 μm.

Fig. 3. MEF2C is required for *Tdgf1* enhancer activity and expression in the heart. (A-D) *Tdgf1::lacZ* (A,B) and *Tdgf1^lacZ/+* (C,D) transgenic embryos crossed onto wild-type (wt) (A,C) or *Mef2c*-null (B,D) backgrounds, collected at E8.5 and X-gal stained. Note the loss of X-gal staining in the absence of *Mef2c* function (B,D). (E) EMSA of a double-stranded radiolabeled oligonucleotide probe encompassing the *Tdgf1* MEF2 site by recombinant MEF2C (lane 2). MEF2C binding was efficiently competed by ∼30-fold excess of unlabeled self probe (lane 3), but was not competed by ∼30-fold excess of a mutant version of the probe (lane 4). Unprogrammed lysate (lacking MEF2C) is shown in lane 1. Bound MEF2C, a non-specific complex (ns) and free probe bands are indicated. (F,G) Representative X-gal-stained E9.5 embryos harboring a wild-type (wt) *Tdgf1::lacZ* transgene (F) and a *Tdgf1::lacZ* transgene with a disrupted MEF2 site (mMEF2) (G). 8/13 *Tdgf1::lacZ*(wt) lines/embryos showed a strong pattern of X-gal staining, such as in the embryo shown in F. By contrast, 2/7 independent *Tdgf1::lacZ*(mMEF2) founder embryos showed weak X-gal staining, such as shown in G, and 5/7 *Tdgf1::lacZ*(mMEF2) founder embryos showed no detectable X-gal staining. Arrows (A-D,F,G) mark the OFT.

expression from the OFT or lower it enough to uncover an OFT phenotype. It is possible that subtle, incompletely penetrant OFT defects might occur, but we observed no evidence of this (data not shown). Considering that the *Mef2c*^AHF-KO phenotype is only ∼50% penetrant on an outbred background (Table 1), failure to observe an overt phenotype in *Mef2c*^+/−*;Tdgf1*^+/− double-heterozygous mice is not surprising and does not diminish the significance of the direct transcriptional relationship between MEF2C and *Tdgf1* identified in these studies. *TDGF1* has been associated with VSDs and OFT alignment defects in humans (Roessler et al., 2008; Wang et al., 2011), but the pathways associated with *TDGF1* in heart development were previously unknown. *MEF2C* has also been
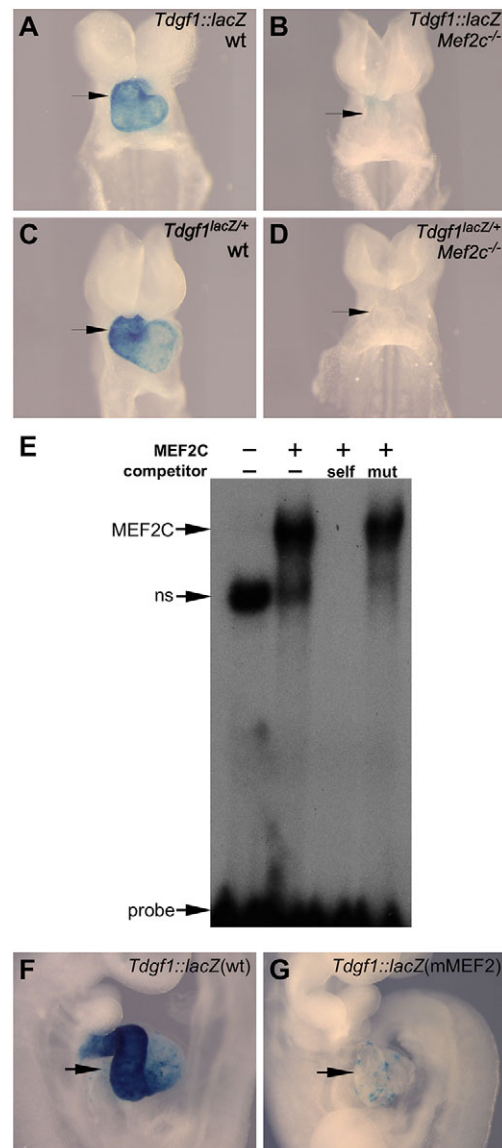
implicated as having a possible role in OFT defects in humans. Kodo et al. (2012) identified a single sequence variant in human *MEF2C* (A103V) in a single patient with isolated congenital heart disease. Although this observation is not conclusive, taken together with the work presented here it supports a role for an *MEF2C*-*TDGF1* pathway in human congenital OFT defects.

Nodal signaling is crucial for the establishment of laterality in the early embryo, and disrupted Nodal signaling has been implicated in human congenital heart disease (Roessler et al., 2008; Shen, 2007). Congenital heart defects due to disrupted Nodal signaling have generally been associated with global defects in left-right patterning, such as heterotaxy (Bisgrove et al., 2003; Mohapatra et al., 2009), but in light of the work presented here it is interesting to speculate that a Nodal signaling network, including TDGF1, might be redeployed later in heart development to achieve local left-right or anteroposterior patterning. Importantly, expression of Nodal ligand-encoding genes, particularly *Gdf1*, continues beyond the time of gastrulation and is present at the time and in the vicinity of the early developing heart (Rankin et al., 2000; Wall et al., 2000). Moreover, several other downstream components of Nodal signaling, including FOXH1 and PITX2C, are also known to play important roles, possibly in a pathway with MEF2C in the AHF (Ai et al., 2006; Furtado et al., 2011; von Both et al., 2004). Alternatively, TDGF1 might function in the OFT in a manner independent of its role as a Nodal co-receptor, possibly as a secreted protein, as has been proposed previously (Yan et al., 2002).

The cellular basis for the OFT shortening in *Mef2c*[AHF-KO] neonates is unclear. It is possible that subtle defects in proliferation, apoptosis or lineage contribution occur in a subset of embryos and that this accounts for the incompletely penetrant phenotype at neonatal stages, but these changes were not apparent when analyzing all mutant embryos. Alternatively, MEF2C might control OFT alignment and elongation via a cellular process or molecular pathway not examined here. Further studies will be required to elucidate additional roles of MEF2C, TDGF1, and their downstream pathways in OFT morphogenesis.

MATERIALS AND METHODS
Mice
Mef2c-AHF-Cre, *Mef2c*[flox/flox], *Mef2c*^{+/−}, *Tdgf1*[lacZ/+] (*Tdgf1*^{+/−}), *Rosa26R* and *Nkx2-5*-null mice have each been described previously (Ding et al., 1998; Lin et al., 1997; Moses et al., 2001; Soriano, 1999; Verzi et al., 2005; Vong et al., 2005). Transgenic mouse lines were generated by oocyte microinjection as described previously (Rojas et al., 2005). To generate *Tdgf1::lacZ* transgenic mice, a 5.21 kb fragment of the *Tdgf1* gene was amplified from mouse genomic DNA using primers 5′-GCCCCGC-GGCAACCTGGGCTACTGATGGT-3′ and 5′-GGCGCGGCCGCGTG-ATTGAGGACTTCGGAGG-3′. The product was then cloned as a *Sac*I-*Not*I fragment into plasmid p-AUG-β-gal (De Val et al., 2008) to make plasmid *Tdgf1-lacZ*, which was then used for subsequent generation of transgenic mice. The MEF2 site mutation was introduced into the full-length 5.21 kb *Tdgf1* enhancer by site-directed mutagenesis using primers 5′-GCCATCTCTCCAGCTGCTGGGATTAAGTTTTTGA-TGCAGATATTTTATGACAGTTG-3′ and 5′-CAACTGTCATAAAATA-TCTGCATCAAAAACTTAATCCCAGCAGCTGGAGAGATGGC-3′. Genotyping was performed on DNA isolated from yolk sacs or from tail biopsies by Southern blot or PCR. All experiments using animals were approved by the UCSF Institutional Animal Care and Use Committee and complied with federal and institutional guidelines.

Histological analyses, X-gal staining and *in situ* hybridization
Section and whole-mount *in situ* hybridization and whole-mount X-gal staining were performed using standard procedures, as previously described (McCulley et al., 2008; Rojas et al., 2005). The *Mef2c* and *Tdgf1* probes have been described elsewhere (Anderson et al., 2015; Ding et al., 1998). Lineage analysis using *Mef2c*-AHF-Cre;*Rosa26R* mice and analyses of apoptosis with anti-cleaved caspase 3 (1:200) and of proliferation with anti-phospho-histone H3 (1:200) were performed as described previously (McCulley et al., 2008; Sinha et al., 2012).

3D reconstructions and measurements
Neonatal hearts were fixed in 4% paraformaldehyde overnight at 4°C and then embedded in paraffin, cut into 5-µm sections, and stained with Hematoxylin and Eosin. Images of consecutive sections were acquired using an Olympus BX40 light microscope and were then stacked and aligned using the Fiji version of ImageJ software. Volume and surface area measurements were taken from 3D reconstructions using Imaris software (Bitplane). Aorta length was measured from the base of the aortic root to the brachiocephalic arterial branch using Fiji.

RNA sequencing (RNA-seq) and quantitative real-time PCR (qPCR)
Embryonic OFTs were collected at E10.5 and RNA was extracted using the RNeasy Micro Kit (Qiagen, 74004) according to the manufacturer's recommendations. cDNA was generated using the Ovation RNA-Seq System V2 (NuGen). cDNA was then fragmented to ~200-300 bp before ligating to barcoded TruSeq adaptors using the Encore Rapid Library System (NuGen). Resulting libraries were sequenced on a HiSeq 2000 (Illumina). FASTQ files were aligned to the reference mouse genome (mm9) using TopHat v1.3 (Trapnell et al., 2009). Differential expression was determined with U-Seq version 8.0.2 (Nix et al., 2008). RNA-seq data have been deposited in the Gene Expression Omnibus repository under accession number GSE68147. qPCR was performed using the SYBR Green system (Life Technologies) using the primers listed in Table S2.

Electrophoretic mobility shift assay (EMSA)
EMSA was performed as described previously (Rojas et al., 2005). MEF2C was transcribed and translated using the TNT Quick Coupled Transcription/Translation System (Promega) from plasmid pCITE-MEF2C, which was made by cloning the *Mef2c* coding sequence in frame into the *in vitro* translation plasmid pCITE-2B (Promega). The sense strand sequences of the *Tdgf1* MEF2 site (underlined) oligonucleotides used for EMSA were: MEF2 site, 5′-GGGATCAAAAACTTAATTTTAGCAGCTGGAG-3′; mutant MEF2 site (changes in bold), 5′-GGGATCAAAAACTTAAT**CCC**AGC-AGCTGGAG-3′.

Supplementary information
Supplementary information available online at
http://dev.biologists.org/lookup/suppl/doi:10.1242/dev.126383/-/DC1

References
Ai, D., Liu, W., Ma, L., Dong, F., Lu, M.-F., Wang, D., Verzi, M. P., Cai, C., Gage, P. J., Evans, S. et al. (2006). Pitx2 regulates cardiac left–right asymmetry by patterning second cardiac lineage-derived myocardium. *Dev. Biol.* **296**, 437-449.
Anderson, R. H., Wilkinson, J. L., Arnold, R., Becker, A. E. and Lubkiewicz, K. (1974). Morphogenesis of bulboventricular malformations. II. Observations on malformed hearts. *Br. Heart J.* **36**, 948-970.

DEVELOPMENT

Anderson, R. H., Spicer, D. E., Giroud, J. M. and Mohun, T. J. (2013). Tetralogy of Fallot: nosological, morphological, and morphogenetic considerations. *Cardiol. Young* **23**, 858-866.

Anderson, C. M., Hu, J., Barnes, R. M., Heidt, A. B., Cornelissen, I. and Black, B. L. (2015). Myocyte enhancer factor 2C function in skeletal muscle is required for normal growth and glucose metabolism in mice. *Skelet. Muscle* **5**, 7.

Behrens, A. N., Ren, Y., Ferdous, A., Garry, D. J. and Martin, C. M. (2012). Nkx2-5 regulates Tdgf1 (Cripto) early during cardiac development. *J. Clin. Exp. Cardiol.* Suppl. 11, 1-4.

Bisgrove, B. W., Morelli, S. H. and Yost, H. J. (2003). Genetics of human laterality disorders: insights from vertebrate model systems. *Annu. Rev. Genomics Hum. Genet.* **4**, 1-32.

Black, B. L. (2007). Transcriptional pathways in second heart field development. *Semin. Cell Dev. Biol.* **18**, 67-76.

Brown, C. B., Wenning, J. M., Lu, M. M., Epstein, D. J., Meyers, E. N. and Epstein, J. A. (2004). Cre-mediated excision of Fgf8 in the Tbx1 expression domain reveals a critical role for Fgf8 in cardiovascular development in the mouse. *Dev. Biol.* **267**, 190-202.

De Val, S., Chi, N. C., Meadows, S. M., Minovitsky, S., Anderson, J. P., Harris, I. S., Ehlers, M. L., Agarwal, P., Visel, A., Xu, S.-M. et al. (2008). Combinatorial regulation of endothelial gene expression by ets and forkhead transcription factors. *Cell* **135**, 1053-1064.

Ding, J., Yang, L., Yan, Y.-T., Chen, A., Desai, N., Wynshaw-Boris, A. and Shen, M. M. (1998). *Cripto* is required for correct orientation of the anterior-posterior axis in the mouse embryo. *Nature* **395**, 702-707.

Dodou, E., Verzi, M. P., Anderson, J. P., Xu, S.-M. and Black, B. L. (2004). Mef2c is a direct transcriptional target of ISL1 and GATA factors in the anterior heart field during mouse embryonic development. *Development* **131**, 3931-3942.

Doetschman, T. (2009). Influence of genetic background on genetically engineered mouse phenotypes. *Methods Mol. Biol.* **530**, 423-433.

Dorfman, A. L. and Geva, T. (2006). Magnetic resonance imaging evaluation of congenital heart disease: conotruncal anomalies. *J. Cardiovasc. Magn. Reson.* **8**, 645-659.

Dubchak, I. and Ryaboy, D. V. (2006). VISTA family of computational tools for comparative analysis of DNA sequences and whole genomes. *Methods Mol. Biol.* **338**, 69-89.

Furtado, M. B., Biben, C., Shiratori, H., Hamada, H. and Harvey, R. P. (2011). Characterization of Pitx2c expression in the mouse heart using a reporter transgene. *Dev. Dyn.* **240**, 195-203.

Hoffman, J. I. E. and Kaplan, S. (2002). The incidence of congenital heart disease. *J. Am. Coll. Cardiol.* **39**, 1890-1900.

Johnson, T. R. (2010). Conotruncal cardiac defects: a clinical imaging perspective. *Pediatr. Cardiol.* **31**, 430-437.

Kelly, R. G. (2012). The second heart field. *Curr. Top. Dev. Biol.* **100**, 33-65.

Kodo, K., Nishizawa, T., Furutani, M., Arai, S., Ishihara, K., Oda, M., Makino, S., Fukuda, K., Takahashi, T., Matsuoka, R. et al. (2012). Genetic analysis of essential cardiac transcription factors in 256 patients with non-syndromic congenital heart defects. *Circ. J.* **76**, 1703-1711.

Lin, Q., Schwarz, J., Bucana, C. and Olson, E. N. (1997). Control of mouse cardiac morphogenesis and myogenesis by transcription factor MEF2C. *Science* **276**, 1404-1407.

McCulley, D. J., Kang, J.-O., Martin, J. F. and Black, B. L. (2008). BMP4 is required in the anterior heart field and its derivatives for endocardial cushion remodeling, outflow tract septation, and semilunar valve development. *Dev. Dyn.* **237**, 3200-3209.

Menon, V., Eberth, J. F., Goodwin, R. L. and Potts, J. D. (2015). Altered hemodynamics in the embryonic heart affects outflow valve development. *J. Cardiovasc. Dev. Dis.* **2**, 108-124.

Mohapatra, B., Casey, B., Li, H., Ho-Dawson, T., Smith, L., Fernbach, S. D., Molinari, L., Niesh, S. R., Jefferies, J. L., Craigen, W. J. et al. (2009). Identification and functional characterization of NODAL rare variants in heterotaxy and isolated cardiovascular malformations. *Hum. Mol. Genet.* **18**, 861-871.

Moses, K. A., DeMayo, F., Braun, R. M., Reecy, J. L. and Schwartz, R. J. (2001). Embryonic expression of an Nkx2-5/Cre gene using ROSA26 reporter mice. *Genesis* **31**, 176-180.

Nakazawa, M., Uchida, K., Aramaki, M., Kodo, K., Yamagishi, C., Takahashi, T., Mikoshiba, K. and Yamagishi, H. (2011). Inositol 1,4,5-trisphosphate receptors

are essential for the development of the second heart field. *J. Mol. Cell. Cardiol.* **51**, 58-66.

Neeb, Z., Lajiness, J. D., Bolanis, E. and Conway, S. J. (2013). Cardiac outflow tract anomalies. *Wiley Interdiscip. Rev. Dev. Biol.* **2**, 499-530.

Nix, D. A., Courdy, S. J. and Boucher, K. M. (2008). Empirical methods for controlling false positives and estimating confidence in ChIP-Seq peaks. *BMC Bioinformatics* **9**, 523.

Racedo, S. E., McDonald-McGinn, D. M., Chung, J. H., Goldmuntz, E., Zackai, E., Emanuel, B. S., Zhou, B., Funke, B. and Morrow, B. E. (2015). Mouse and human CRKL is dosage sensitive for cardiac outflow tract formation. *Am. J. Hum. Genet.* **96**, 235-244.

Rana, M. S., Theveniau-Ruissy, M., De Bono, C., Mesbah, K., Francou, A., Rammah, M., Dominguez, J. N., Roux, M., Laforest, B., Anderson, R. H. et al. (2014). Tbx1 coordinates addition of posterior second heart field progenitor cells to the arterial and venous poles of the heart. *Circ. Res.* **115**, 790-799.

Rankin, C. T., Bunton, T., Lawler, A. M. and Lee, S.-J. (2000). Regulation of left-right patterning in mice by growth/differentiation factor-1. *Nat. Genet.* **24**, 262-265.

Roessler, E., Ouspenskaia, M. V., Karkera, J. D., Velez, J. I., Kantipong, A., Lacbawan, F., Bowers, P., Belmont, J. W., Towbin, J. A., Goldmuntz, E. et al. (2008). Reduced NODAL signaling strength via mutation of several pathway members including FOXH1 is linked to human heart defects and holoprosencephaly. *Am. J. Hum. Genet.* **83**, 18-29.

Rojas, A., De Val, S., Heidt, A. B., Xu, S.-M., Bristow, J. and Black, B. L. (2005). Gata4 expression in lateral mesoderm is downstream of BMP4 and is activated directly by Forkhead and GATA transcription factors through a distal enhancer element. *Development* **132**, 3405-3417.

Schier, A. F. and Shen, M. M. (2000). Nodal signalling in vertebrate development. *Nature* **403**, 385-389.

Shen, M. M. (2007). Nodal signaling: developmental roles and regulation. *Development* **134**, 1023-1034.

Shen, M. M. and Schier, A. F. (2000). The EGF-CFC gene family in vertebrate development. *Trends Genet.* **16**, 303-309.

Sinha, T., Wang, B., Evans, S., Wynshaw-Boris, A. and Wang, J. (2012). Disheveled mediated planar cell polarity signaling is required in the second heart field lineage for outflow tract morphogenesis. *Dev. Biol.* **370**, 135-144.

Soriano, P. (1999). Generalized *lacZ* expression with the ROSA26 Cre reporter strain. *Nat. Genet.* **21**, 70-71.

Thurman, R. E., Rynes, E., Humbert, R., Vierstra, J., Maurano, M. T., Haugen, E., Sheffield, N. C., Stergachis, A. B., Wang, H., Vernot, B. et al. (2012). The accessible chromatin landscape of the human genome. *Nature* **489**, 75-82.

Trapnell, C., Pachter, L. and Salzberg, S. L. (2009). TopHat: discovering splice junctions with RNA-Seq. *Bioinformatics* **25**, 1105-1111.

Verzi, M. P., McCulley, D. J., De Val, S., Dodou, E. and Black, B. L. (2005). The right ventricle, outflow tract, and ventricular septum comprise a restricted expression domain within the secondary/anterior heart field. *Dev. Biol.* **287**, 134-145.

Vincentz, J. W., McWhirter, J. R., Murre, C., Baldini, A. and Furuta, Y. (2005). Fgf15 is required for proper morphogenesis of the mouse cardiac outflow tract. *Genesis* **41**, 192-201.

von Both, I., Silvestri, C., Erdemir, T., Lickert, H., Walls, J. R., Henkelman, R. M., Rossant, J., Harvey, R. P., Attisano, L. and Wrana, J. L. (2004). Foxh1 is essential for development of the anterior heart field. *Dev. Cell* **7**, 331-345.

Vong, L. H., Ragusa, M. J. and Schwarz, J. J. (2005). Generation of conditional Mef2cloxP/loxP mice for temporal- and tissue-specific analyses. *Genesis* **43**, 43-48.

Wall, N. A., Craig, E. J., Labosky, P. A. and Kessler, D. S. (2000). Mesendoderm induction and reversal of left–right pattern by mouse Gdf1, a Vg1-related gene. *Dev. Biol.* **227**, 495-509.

Wang, B., Yan, J., Peng, Z., Wang, J., Liu, S., Xie, X. and Ma, X. (2011). Teratocarcinoma-derived growth factor 1 (TDGF1) sequence variants in patients with congenital heart defect. *Int. J. Cardiol.* **146**, 225-227.

Xu, C., Liguori, G., Persico, M. G. and Adamson, E. D. (1999). Abrogation of the Cripto gene in mouse leads to failure of postgastrulation morphogenesis and lack of differentiation of cardiomyocytes. *Development* **126**, 483-494.

Yan, Y.-T., Liu, J.-J., Luo, Y., E, C., Haltiwanger, R. S., Abate-Shen, C. and Shen, M. M. (2002). Dual roles of Cripto as a ligand and coreceptor in the nodal signaling pathway. *Mol. Cell. Biol.* **22**, 4439-4449.

DEVELOPMENT